

Article

Comparison of Nutritional and Medicinal Ingredients Between *Ganoderma leucocontextum* and *G. lucidum*

Peng Wang ^{1,†}, Fei Fang ^{1,†}, Chunxin Yao ² , Qian Teng ¹, Guoting Tian ², Linhai Hong ¹, Yalan Bin ¹ and Qinghong Liu ^{1,*} 

¹ Department of Vegetables, College of Horticulture, China Agricultural University, Haidian District, Beijing 100193, China; wangpeng_1998@cau.edu.cn (P.W.); hardff@cau.edu.cn (F.F.); tengqian980@cau.edu.cn (Q.T.); hlh@cau.edu.cn (L.H.); binyi101@cau.edu.cn (Y.B.)

² Biotechnology and Genetic Germplasm Resources Research Institute, Yunnan Academy of Agricultural Sciences, Kunming 650205, China; ycx@yaas.org.cn (C.Y.); tgt@yaas.org.cn (G.T.)

* Correspondence: qhliu@cau.edu.cn

† These authors contributed equally to this work.

Abstract: The genus *Ganoderma* is a widely used medicinal fungus in East Asia. The main medicinal components are triterpenoids, polyphenols, and polysaccharides. Bitterness is an important commercial trait for *Ganoderma*. White Lingzhi (*G. leucocontextum*) is less bitter. But the characteristics of its nutritional and medicinal ingredients are still unclear, which undoubtedly limits its commercialization. In this study, the medicinal ingredients of Lingzhi and white Lingzhi were extracted and quantified. The structure and antioxidant activities of purified polysaccharides were determined. At the same time, their nutritional differences were compared. White Lingzhi contains more medicinal ingredients and its polysaccharide is more active. The higher protein content may be one of the reasons for weaker bitterness in white Lingzhi. The nutritional and medicinal traits of white Lingzhi were described for the first time in this study, which provides fundamental knowledge to support the development of white Lingzhi.

Keywords: white Lingzhi; Lingzhi; Chinese traditional medicine



Citation: Wang, P.; Fang, F.; Yao, C.; Teng, Q.; Tian, G.; Hong, L.; Bin, Y.; Liu, Q. Comparison of Nutritional and Medicinal Ingredients Between *Ganoderma leucocontextum* and *G. lucidum*. *Agronomy* **2024**, *14*, 2523. <https://doi.org/10.3390/agronomy14112523>

Academic Editor: Mark P. Widrlechner

Received: 13 September 2024

Revised: 24 October 2024

Accepted: 25 October 2024

Published: 27 October 2024



Copyright: © 2024 by the authors. Licensee MDPI, Basel, Switzerland. This article is an open access article distributed under the terms and conditions of the Creative Commons Attribution (CC BY) license (<https://creativecommons.org/licenses/by/4.0/>).

1. Introduction

Ganoderma lucidum, commonly known as Lingzhi, is a traditional Chinese fungus that is widely used in China, Japan, Korea, and other Asian countries. It possesses a wide range of bioactivities, including anti-tumor properties [1,2], immunomodulatory effects [3], antimicrobial and antiviral activities [4], liver-protective effects [5], anti-aging properties [6], and potential in diabetes control [7]. Lingzhi has been extensively studied due to its numerous beneficial properties.

In 2015, *G. leucocontextum*, also known as white Lingzhi, was identified as a new species [8]. White Lingzhi exhibits significant morphological differences compared to Lingzhi. While Lingzhi has a semi-circular or kidney-shaped cap and off-white to light brown hard flesh, white Lingzhi has a semi-circular or fan-shaped cap and white soft flesh. Additionally, white Lingzhi has been found to promote neurite outgrowth [9] and possess immunomodulatory effects [10].

The medicinal value of *Ganoderma* fungi primarily stems from the presence of bioactive substances, including polysaccharides, triterpenoids, polyphenols, and proteins [11]. However, Lingzhi's practical applications are hindered by its poor palatability due to its strong bitter taste. Furthermore, there have been reports of adverse reactions associated with Lingzhi consumption, such as dry mouth, nausea [12], diarrhea [13], sore throat [14], and insomnia [1].

In contrast, white Lingzhi exhibits relatively less bitterness and causes milder hypersensitivity reactions, making it a more promising candidate for broader applications.

These characteristics of white Lingzhi make it more palatable and tolerable for individuals, potentially increasing its acceptability and usage.

Overall, the discovery of white Lingzhi as a new species and its distinct morphological features, along with its unique bioactivities, suggest that white Lingzhi has the potential to contribute to the development of new therapeutic agents. Further research is warranted to explore the full range of its medicinal properties and potential applications.

In this study, our focus was on examining differences in the main nutritional and medicinal ingredients between white Lingzhi and Lingzhi. We extracted the main medicinal ingredients and quantified these medicinal and nutritional components. Additionally, we characterized the structure of the polysaccharide. Furthermore, to gain a clearer understanding of the bioactivities, we investigated the antioxidant capacity *in vitro* of the polysaccharides, phenolics, and triterpenoids.

These investigations into the differences between white Lingzhi and Lingzhi may explain the milder and less bitter taste of white Lingzhi. The details obtained from this study will serve as a foundation for the more accurate application of white Lingzhi, providing valuable insights into its potential benefits and uses.

2. Materials and Methods

2.1. Materials and Chemicals

Fresh fruiting bodies of Lingzhi and white Lingzhi were collected from the Biotechnology and Genetic Germplasm Resources Research Institute, Kunming, China. 1,1-diphenyl-2-picrylhydrazyl (DPPH), pyrogalllic acid, and ferrozine were obtained from Sigma-Aldrich. All the reagents were analytical grade.

2.2. Preparation of Sample

The fruiting bodies were dried in an oven at 40 °C until a constant weight was achieved. Subsequently, they were ground into a fine powder (40 mesh) using a ball mill (model PM 100; Retsch GmbH; Haan, Germany) operating at a speed of 350 rpm for 1.5 h. The ball mill operated for 5 min followed by a 10 min interval during which the rotational direction was changed. These powder samples were stored in a desiccator for the following experiments.

2.3. Determination of Protein Content

The content of crude protein was quantified by the Kjeldahl method [15]. A total of 1 g sample of powder was mixed with 12 mL H₂SO₄ and 6.4 g catalytic mix (K₂SO₄:CuSO₄ = 15:1, *w/w*). The sample was heated to 400 °C to completely fix the protein nitrogen into ammonium. In total, 60 mL H₂O and 50 mL 40% NaOH solution were added to the digestion solution and heated for distillation. The distillate was absorbed by 2.5% H₃BO₃, which was then titrated with 0.05 mol/L HCl standardized for the quantification of total nitrogen (N). For the protein content, the value of N was converted to N × 4.38 fungal protein [16].

2.4. Determination of Amino Acids Composition

The amino acid composition was determined by the ninhydrin method with minor modification [17]. The sample (50 mg) was hydrolyzed by 6 M HCl for 24 h at 110 °C *in vacuo*. The supernatant was transferred and concentrated after cooling in the dark. The concentrated solution was diluted with sodium citrate buffer (0.2 M, pH 2.2) and filtered through a 0.2 µm filter for analysis via an amino acid analyzer (Biochrom; Cambridge, UK). A mixture of 17 kinds of amino acids was used as a working standard. The concentration of each amino acid was 100 nmol/mL. The content of valine was determined by an HPLC system equipped with a C18 column and UV detector. Tryptophan content was determined using the p-dimethylaminobenzaldehyde (p-DAB) colorimetric method [18].

2.5. Determination of Triterpenoid Content

Triterpenoids were extracted using methanol as the solvent. The sample was evenly dispersed in methanol at a ratio of 1:10 (*w/v*). The mixture was then shaken for 12 h at room temperature to ensure complete extraction.

The content of total triterpenoids (Tr) was represented by ursolic acid equivalents [19]. In brief, 100 μ L of the extracting solution was mixed with 150 μ L of 5% vanillin solution (dissolved in glacial acetic acid) and 500 μ L of a 70% perchloric acid solution. The resulting mixture was heated for 45 min at 60 °C and then cooled on ice. As it cooled, 2.25 mL glacial acetic acid was added. The absorbance of the solution was measured at 548 nm against a blank (methanol). To prepare a calibration curve, different concentrations of ursolic acid (ranging from 0.1 to 0.5 mg/mL) dissolved in methanol were used as standards.

2.6. Determination of Phenolic Content

Phenolics were extracted using methanol as the solvent. The sample was evenly dispersed in methanol at a ratio of 1:10 (*w/v*), and the mixture was shaken for 12 h to ensure full extraction.

The content of total phenolics (Ph) was represented by gallic acid equivalents [20]. A total of 500 μ L of the extract solution was mixed with 2.5 mL of Folin–Ciocalteu reagent (previously diluted ten times in water) and 2.0 mL of Na₂CO₃ solution (75 g/L). The mixture was vortexed and incubated for 30 min at 40 °C to develop color. The absorbance of the solution was measured at 765 nm against a methanol blank. To prepare a calibration curve, different concentrations of gallic acid (ranging from 0.1 to 0.5 mg/mL) dissolved in methanol were used as standards.

2.7. Analysis of Polysaccharide

2.7.1. Extraction of Crude Polysaccharide

The sample powder was dispersed in water at a ratio of 1:15 (*w/v*) and heated at 95 °C for 4 h. After centrifugation at 8000 rpm for 15 min, the supernatant was mixed with ethanol at a ratio of 1:3 (*v/v*) and left to stand for 10 h. The sediment was collected by centrifugation and dissolved in water. To remove proteins, Sevage reagent was used [21].

The polysaccharide content of the supernatant was determined using the 3,5-dinitrosalicylic (DNS) colorimetric method, as described by [22]. Prior to analysis, the supernatant was dialyzed against water by using a membrane with a molecular weight cutoff of 3500 Dalton. The dialyzed solution was then subjected to the DNS colorimetric method to quantify the polysaccharide content.

2.7.2. Purification of Polysaccharide

The polysaccharides were purified following the protocols of Feng et al. [23]. After dialysis against phosphate buffer (0.05 M, pH 7.4), the crude polysaccharide was purified on a DEAE-Sepharose column. Elution was performed stepwise with phosphate buffer (0.05 M, pH 7.4), 0.15 M NaCl in phosphate buffer (0.05 M, pH 7.4), 0.5 M NaCl in phosphate buffer (0.05 M, pH 7.4), and 1 M NaCl in phosphate buffer (0.05 M, pH 7.4). The fractions with high polysaccharide content, eluted by phosphate buffer (0.05 M, pH 7.4) and 0.5 M NaCl in phosphate buffer (0.05 M, pH 7.4), were collected for further analysis.

Subsequently, the collected fractions were subjected to a CM-Sepharose column and eluted with acetate buffer (0.05 M, pH 4.6). The unbound fraction was collected and subsequently freeze-dried to obtain pure polysaccharides. This purification process ensured the isolation of polysaccharides with high purity from the crude extract.

2.7.3. Characterization of Polysaccharide

The molecular weight of the polysaccharide was determined using high-performance gel permeation chromatography (HPGPC) with an Agilent 1200 HPLC system equipped with a PL aquagel-OH 50 column (7.7 \times 300 mm) and a differential refractive index detector following the method described by [24]. Phosphate buffer (0.2 M, pH 7.5) was used as the

flow phase at a flow rate of 0.5 mL/min. The weight-average molecular weights (Mw) and number-average molecular weights (Mn) were estimated from a calibration equation based on PL pullulan polysaccharide standards.

A thermogravimetric analysis (TGA) of polysaccharide was conducted with a thermal analyzer (model STA 2500; Netzsch; Selb, Germany) under a nitrogen atmosphere, and heated from 30 to 800 °C with a heating rate of 10 °C/min [25].

The polysaccharide was hydrolyzed by trifluoroacetic acid (TFA, 2.0 M) [26] and then analyzed using a high-performance anion exchange chromatography (HPAEC) system (Dionex ISC 3000, Sunnyvale, CA, USA) with pulsed amperometric detector (PAD), CarboPac PA20 column (4 × 250 mm, Dionex), and PA-20 guard column (3 × 30 mm). Calibration was performed using the standard solutions of L-arabinose, D-xylose, D-glucose, D-mannose, D-galactose, glucuronic acid, and galacturonic acid.

Fourier-transform infrared spectroscopy (FTIR) was performed on an FTIR spectrometer (Alpha; Bruker; Optics, Germany) with KBr disks containing 1% finely ground samples [27]. The spectrum was recorded in the range of 4000 to 400 cm⁻¹.

For nuclear magnetic resonance (NMR) spectroscopy, the polysaccharide was dissolved in D₂O, and solution-state ¹H, ¹³C, and heteronuclear single quantum coherence (HSQC) NMR spectra were acquired at 298 K from an Avance III HD 500 spectrometer (Bruker; Optics, Germany) [28].

2.8. Antioxidant Capacity In Vitro

In this experiment, polysaccharides and phenolics were dissolved in phosphate buffer (0.1 M, pH 7.4), while triterpenoids were dissolved in 50% methanol. Antioxidant capacity was determined as follows:

The ability to scavenge H₂O₂ was evaluated following [29] with minor modifications. Sample solution (1.0 mL) with different concentrations was added to a mixture containing 0.4 mL H₂O₂ (0.3%) and 2.0 mL phosphate buffer (0.1 M, pH 7.4). The absorbance of H₂O₂ at 230 nm was determined after 10 min. H₂O₂ scavenging ability = $(A - A_s + A_c)/A \times 100$, where A was the absorbance of the reaction solution without the sample, A_s was the absorbance of the reaction solution with the sample and A_c was that of the solution replaced H₂O₂ with solvent.

DPPH radical scavenging activity was assayed following [30]. Sample solution (1 mL) with different concentrations was added to 3 mL 75 µM DPPH in 50% methanol solution. The mixture was kept in the dark at room temperature for 30 min. Absorbance was measured at 517 nm. DPPH scavenging ability (%) = $(A - A_s + A_c)/A \times 100$, where A was the absorbance of the solution including DPPH and methanol, A_s was the absorbance of the sample and DPPH solution, and A_c was the absorbance of the solution including the sample and methanol.

The binding of Fe²⁺ was assessed following [31] with minor modification. Sample solution (800 µL) with different concentrations was added to a reaction mixture containing 2.0 mL deionized water, 40 µL FeCl₂ (2 mM), and 160 µL ferrozine solution (5 mM). Absorbance at 562 nm was determined after 10 min. The binding rate of Fe²⁺ = $(A - A_s + A_c)/A \times 100$, where A was the absorbance of the reaction solution without the sample, A_s was the absorbance of the reaction solution with the sample, and A_c was that of the solution including the sample and water only.

2.9. Statistical Analysis

The independent experiments were performed in triplicate, and all the data were expressed as Means ± Standard Deviation (M ± S.D.). Statistical analyses were performed by one-way ANOVA using the software program GraphPad Prism 8.0. The FTIR and TGA spectra were plotted with Origin 2019. The NMR spectra were analyzed with the software program MestreNova 14.0.

3. Results

3.1. Difference in Crude Protein Concentration

The crude protein concentration of white Lingzhi was 11.98%, while Lingzhi was only 8.98% (Figure 1). In a wider study of Chinese Lingzhi, the mean protein concentration was 9.9% [32], which falls between our values for Lingzhi and white Lingzhi.

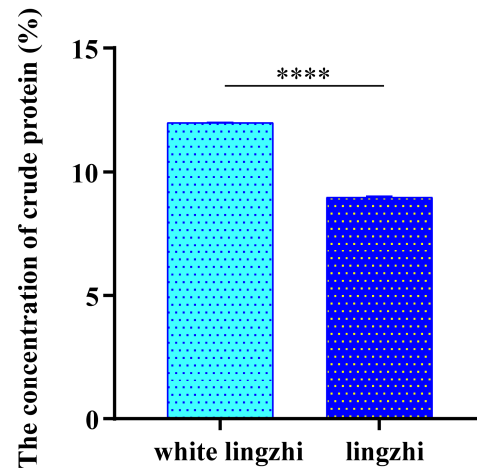


Figure 1. Crude protein concentration in white Lingzhi and Lingzhi. **** indicates that $p < 0.0001$.

3.2. Differences in Amino Acid Composition

For a more detailed comparison of protein, the amino acid compositions were determined. We classified 18 amino acids into four groups (Table 1). The total amino acid concentration of white Lingzhi exceeded that of Lingzhi, which was consistent with the protein results. There were differences in the relative proportions of amino acids. The concentrations of monosodium glutamate-like (MSG-like) amino acids were higher in white Lingzhi, while the overall percentage of sweet amino acids was the highest in Lingzhi. However, there was no significant difference in the relative proportions of the four amino acid groups.

Table 1. Amino acid composition of white Lingzhi and Lingzhi.

Amino Acid		Amino Acid Concentration (mg g ⁻¹)	
		White Lingzhi	Lingzhi
MSG-like	Aspartic acid	0.96 ± 0.02	0.77 ± 0.02
	Glutamic acid	1.44 ± 0.02	0.80 ± 0.02
	Total/percentage	2.40/25.2%	1.57/22.6%
Sweet	Alanine	0.64 ± 0.00	0.50 ± 0.01
	Glycine	0.50 ± 0.01	0.40 ± 0.02
	Serine	0.47 ± 0.01	0.40 ± 0.02
	Threonine	0.51 ± 0.01	0.47 ± 0.02
	Total/percentage	2.12/22.3%	1.77/25.4%
Bitter	Arginine	0.65 ± 0.02	0.32 ± 0.01
	Histidine	0.17 ± 0.00	0.13 ± 0.01
	Leucine	0.88 ± 0.01	0.69 ± 0.02
	Phenylalanine	0.45 ± 0.00	0.34 ± 0.01
	Methionine	0.15 ± 0.01	0.10 ± 0.00
	Cysteine	0.15 ± 0.00	0.18 ± 0.00
	Valine	0.60 ± 0.01	0.48 ± 0.01
	Total/percentage	3.05/32.0%	2.24/32.2%

Table 1. Cont.

Amino Acid		Amino Acid Concentration (mg g ⁻¹)	
		White Lingzhi	Lingzhi
Tasteless	Isoleucine	0.44 ± 0.01	0.35 ± 0.01
	Lysine	0.55 ± 0.01	0.36 ± 0.01
	Proline	0.47 ± 0.01	0.35 ± 0.01
	Tryptophan	0.15 ± 0.001	0.09 ± 0.00
	Tyrosine	0.34 ± 0.00	0.23 ± 0.01
	Total/percentage	1.95/20.5%	1.38/19.8%
Total amino acids		9.52	6.96

3.3. Differences in Concentrations and Antioxidant Activities of Triterpenoids

Triterpenoid concentrations and DPPH scavenging ability are shown in Figure 2. The triterpenoid concentration of white Lingzhi was significantly higher than that of Lingzhi. *Ganoderma* triterpenoids were strong scavengers on DPPH. However, these two triterpenoid extracts showed little activity in H₂O₂ removal or Fe²⁺ chelation. This may be due to the location of the hydroxyl group in their structure. And, it indicates that the mode of action of triterpenoids does not involve Fe²⁺ chelation to any significant degree.

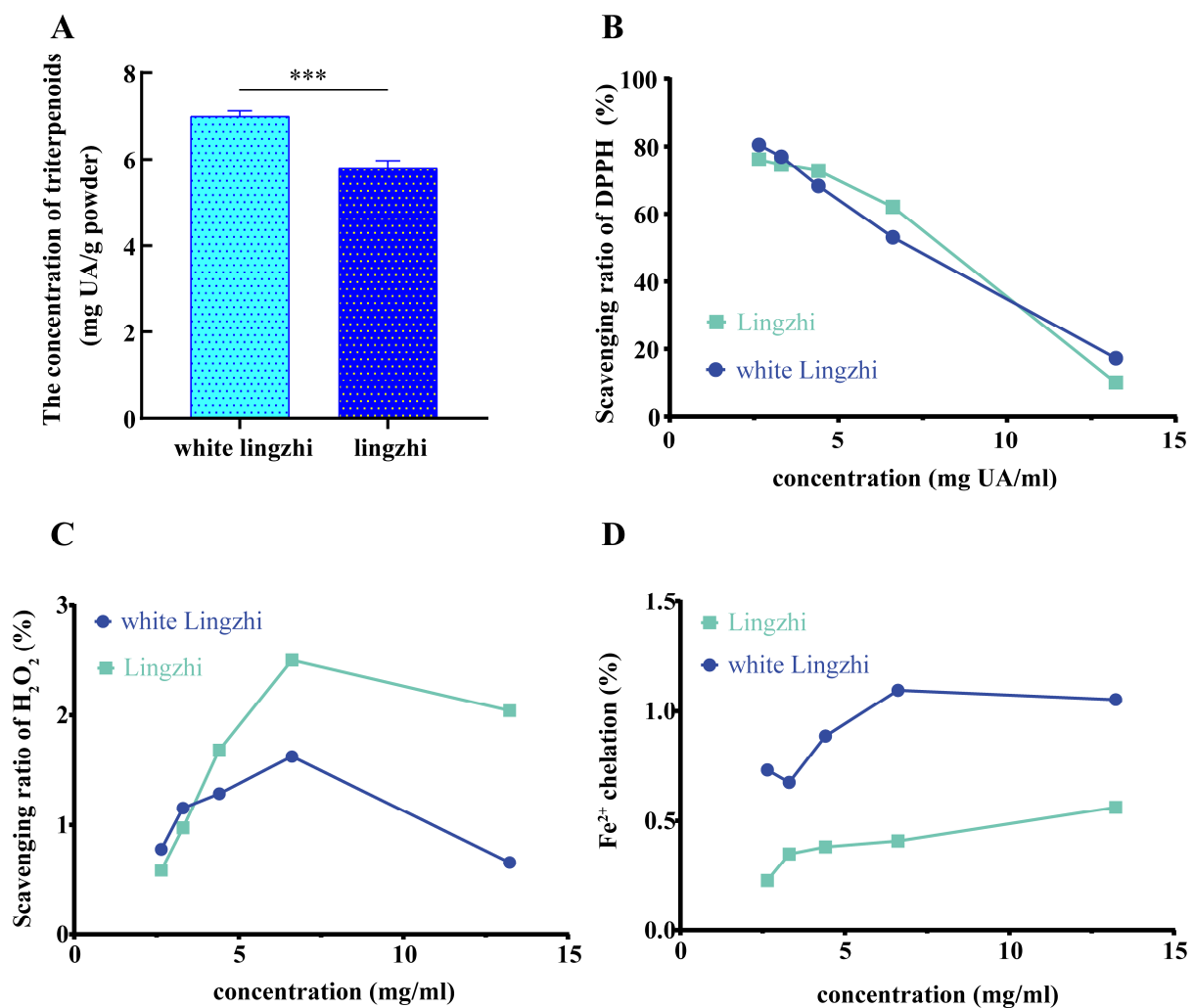


Figure 2. Concentrations and antioxidant activities of triterpenoids. The concentration (A) of triterpenoids and capacity to scavenging DPPH (B), H₂O₂ (C) and chelate Fe²⁺ (D) in white Lingzhi and Lingzhi. *** indicates that $p < 0.001$.

3.4. Differences in Concentrations and Antioxidant Activities of Total Phenolics

No significant difference in the concentration of phenolics between white Lingzhi and Lingzhi was observed. These phenolics are able to scavenge DPPH and H_2O_2 and can chelate Fe^{2+} . But, the relationships between antioxidant capability and concentration were inconsistent. Compared with the phenolics from Lingzhi, those from white Lingzhi had a stronger initial capacity to scavenge H_2O_2 and chelate Fe^{2+} . In addition, the scavenging ability of white Lingzhi phenolics on DPPH was relatively stable, and less affected by their concentration (Figure 3).

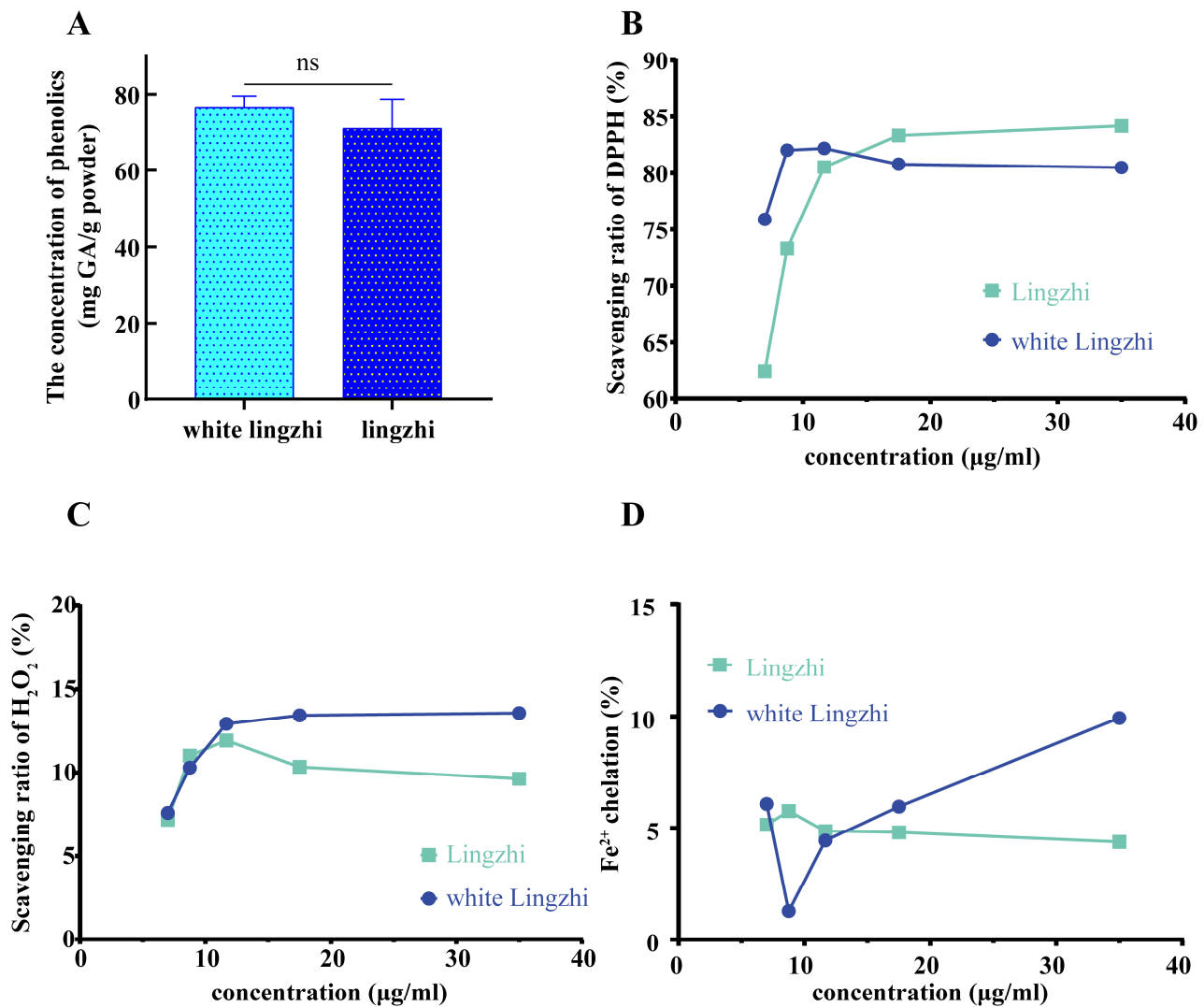


Figure 3. Concentrations and antioxidant activities of phenolics. The concentration (A) of phenolics and capacity to scavenging DPPH (B), H_2O_2 (C) and chelate Fe^{2+} (D) in white Lingzhi and Lingzhi. ns indicates that no significance.

3.5. Differences in Characters and Antioxidant Activities of Polysaccharides

A DEAE-sepharose column was used to separate the polysaccharides into acidic and neutral fractions. The fraction bound to the column was identified as an acidic polysaccharide, while the unbound fraction was identified as a neutral polysaccharide. The purified fractions will be referred to as white Lingzhi neutral polysaccharide (WLNP), white Lingzhi acidic polysaccharide (WLAP), Lingzhi neutral polysaccharide (LNP), and Lingzhi acidic polysaccharide (LAP).

3.5.1. The Molecular Weights of Polysaccharides

Table 2 presents the molecular weights (Mw and Mn) of the four polysaccharides. The polydispersity (PD) values ranged between 1.55 and 1.75, indicating that the molecular weights of the polysaccharides were relatively uniform. Furthermore, it can be observed from Table 2 that the molecular weight of the neutral polysaccharide was higher than that of the acidic polysaccharide.

Table 2. Molecular weight of polysaccharides.

Polysaccharide	Mw	Mn	PD
WLNP	131,127	76,372	1.72
WLAP	123,869	74,105	1.67
LNP	139,141	88,465	1.57
LAP	104,006	61,417	1.69

Note: WLNP, white Lingzhi neutral polysaccharide; WLAP, white Lingzhi acidic polysaccharide; LNP, Lingzhi neutral polysaccharide; and LAP, Lingzhi acidic polysaccharide. PD is an abbreviation for polydispersity and is calculated as the ratio of Mw to Mn.

3.5.2. Thermogravimetric Analysis

The thermal stability of biomolecules plays a vital role in their suitability for various biological applications. In this study, the thermogravimetry (TG) and derivative thermogravimetry (DTG) curves of four polysaccharides were examined, as depicted in Figure 4. As the temperature increased, the residues gradually decreased. Interestingly, the acidic polysaccharides exhibited higher residue levels than did neutral polysaccharides at 800 °C. Moreover, the DTG curves of all four polysaccharides displayed a peak below 100 °C, which can be attributed to the evaporation of residual moisture [33]. However, it is worth noting that the weight loss peak for the acidic polysaccharides was smaller, indicating weaker water absorption and retention capabilities compared to the neutral polysaccharides. The remaining peaks observed in the curves were a result of thermal decomposition [34]. Notably, the thermal decomposition pattern differed between the acidic and neutral polysaccharides. The neutral polysaccharides exhibited significant weight loss between 150 and 400 °C, whereas the acidic polysaccharides displayed a minor, but more abrupt weight loss between 200 and 300 °C, followed by further weight loss above 700 °C. Our TG findings suggest that the acidic polysaccharides possess greater stability at high temperatures. Additionally, when comparing the amount of residues at 800 °C, it was observed that the white Lingzhi polysaccharide exhibited slightly better stability, although the difference was not statistically significant.

3.5.3. Monosaccharide Components of Polysaccharides

Based on our HPAEC-PAD analyses, the composition of the acidic polysaccharide was very simple, while the neutral polysaccharides were more complex (Table 3). The four polysaccharides were mostly composed of glucose (Glc), strongly suggesting that it is the major unit of the main backbone for *Ganoderma* polysaccharides. In addition, the neutral polysaccharides were composed of a large variety of monosaccharides, which suggests they may have a wider range of biological activities. The proportion of Glc in white Lingzhi was lower, with greater balance among the various component monosaccharides, which may be one of the reasons for the mild pharmacological properties of white Lingzhi.

Table 3. The monosaccharide components of polysaccharides.

Sample	Fucose (Fuc)	Galactose (Gal)	Glucose (Glc)	Xylose (Xyl)	Glucuronic Acid (GlcA)
LAP	0.00	0.00	78.07%	0.00	21.93%
WLAP	0.00	0.00	66.91%	0.00	33.09%

Table 3. Cont.

Sample	Fucose (Fuc)	Galactose (Gal)	Glucose (Glc)	Xylose (Xyl)	Glucuronic Acid (GlcA)
LNP	3.65%	12.79%	70.84%	7.51%	5.21%
WLNP	5.05%	19.21%	66.32%	6.00%	3.42%

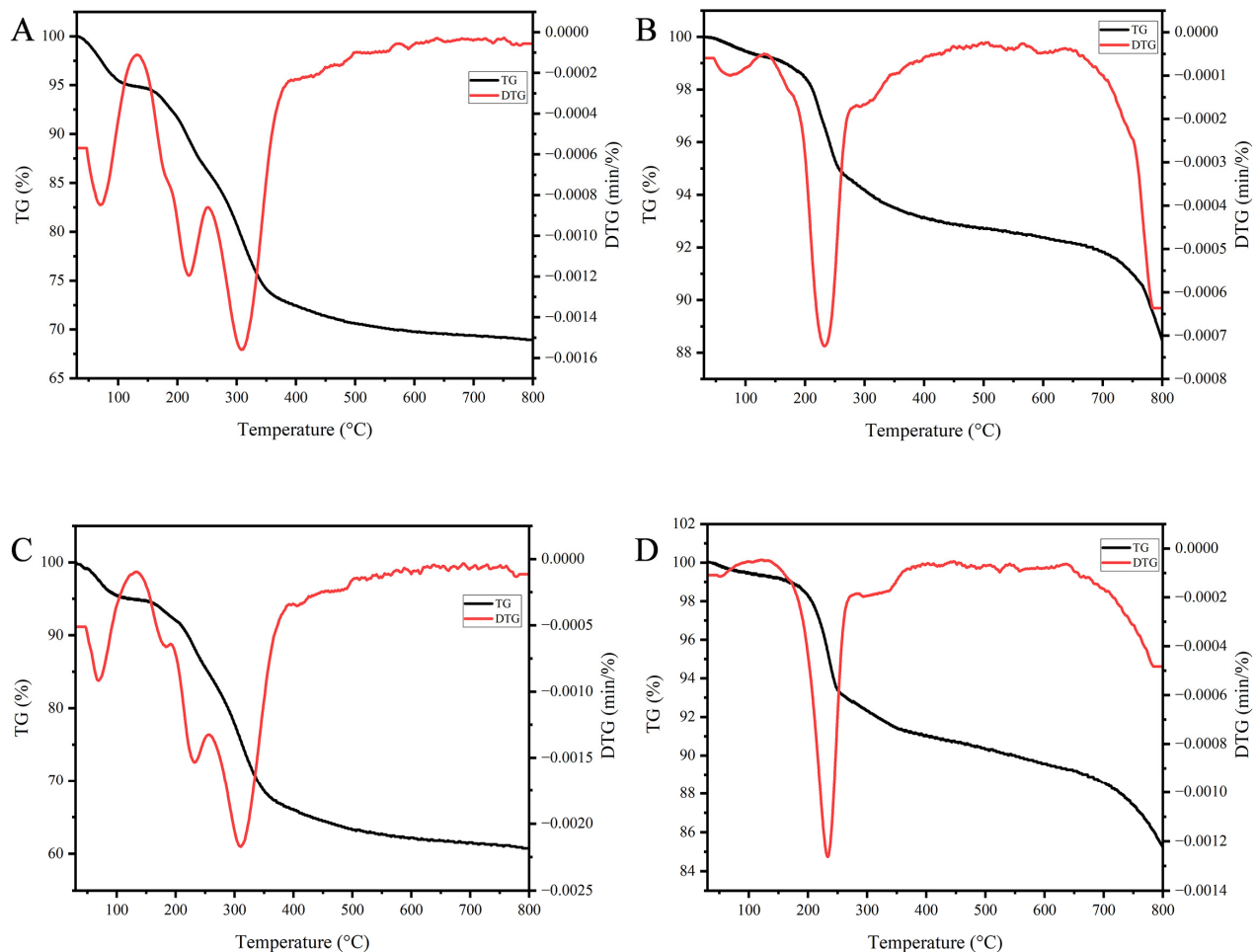


Figure 4. TG and DTG curves for four different samples: (A) WLNP, white Lingzhi neutral polysaccharide; (B) WLAP, white Lingzhi acidic polysaccharide; (C) LNP, Lingzhi neutral polysaccharide; and (D) LAP, Lingzhi acidic polysaccharide.

3.5.4. Polysaccharide Structural Analysis

The structure of the polysaccharides was analyzed using the Fourier-transform infrared spectroscopy (FTIR) and nuclear magnetic resonance (NMR) techniques. The FTIR spectra, presented in Figure 5, facilitate the determination of the chemical bonds and molecular structure of the polysaccharides, serving as complementary methods for structural analysis [35].

Several absorption peaks were observed in the FTIR spectra. The peaks at 3444.24 cm^{-1} and 2891.74 cm^{-1} can be attributed to the stretching vibration of hydroxyl groups and C-H groups, respectively [36,37]. The absorption peaks within the $1700\text{--}1300\text{ cm}^{-1}$ range indicate the presence of carboxyl groups in the polysaccharides. Specifically, the peak at 1635 cm^{-1} reflects C=O linkages [38], while the peak at 1362 cm^{-1} corresponds to carboxylate groups [39]. The peak observed at 1159 cm^{-1} reflects the stretching of α -(1,4) glycosidic linkages [40]. Additionally, the peak at 1074 cm^{-1} confirms the presence of a pyranose ring structure. Furthermore, the peaks observed at 946 cm^{-1} , 861 cm^{-1} , and 547 cm^{-1} represent

β -glycosidic bonds, α -glycosidic bonds, and in-plane C=O bending, respectively [41–43]. Notably, the α -glucosidic bonds in the neutral polysaccharide were not clearly evident in the FTIR spectra.

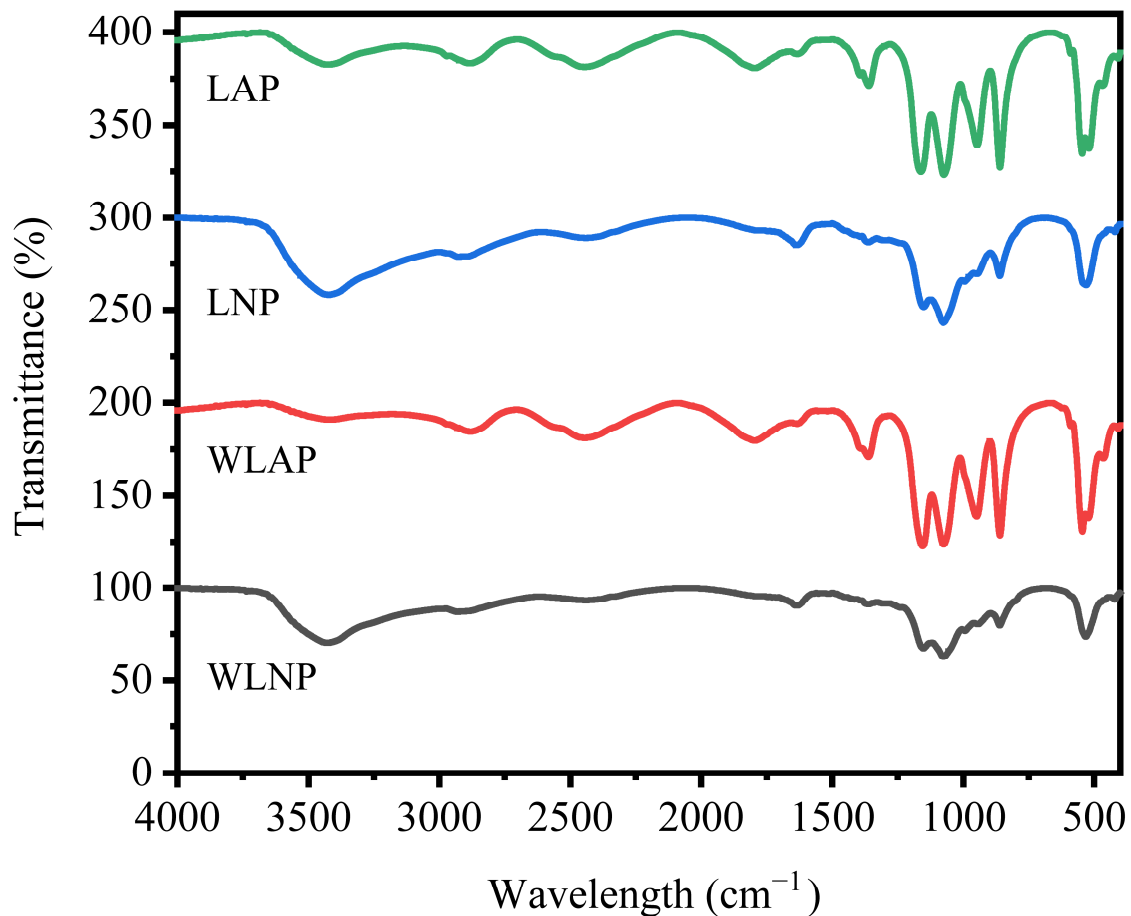


Figure 5. FTIR spectra of WLNP (white Lingzhi neutral polysaccharide), WLAP (white Lingzhi acidic polysaccharide), LNP (Lingzhi neutral polysaccharide), and LAP (Lingzhi acidic polysaccharide).

In summary, the FTIR analysis provided valuable insights into the chemical bonds and molecular structure of the polysaccharides, highlighting the presence of hydroxyl groups, C-H groups, carboxyl groups, α -(1,4) glycosidic linkages, and various other functional groups.

The NMR spectra provide detailed information about the structural characteristics of the polysaccharide polymers. Both the ^1H NMR and HSQC NMR spectra are presented in Figure 6. The ^1H NMR spectra reveal several signals that indicate the presence of specific sugar residues. These include β -D-glucose (3.57 and 3.65 ppm), β -D-mannose (3.76 ppm), α -L-arabinitol (4.12 ppm), and β -D-xylan (4.44 and 3.23 ppm). Further details can be observed in the HSQC spectra.

In the HSQC spectra, a $\delta_{\text{C}}/\delta_{\text{H}}$ signal at 3.83/60.64 ppm corresponds to the C6-H of (1 \rightarrow 4)-linked α -D-glucan [44]. The presence of different Glc configurations in the polysaccharide is evident from the $^1\text{H}/^{13}\text{C}$ chemical shifts. The signals at $\delta_{\text{C}}/\delta_{\text{H}}$ 3.44/72.96 and 3.65/60.74 ppm are assigned to H-5/C-5 and H-6/C-6 of \rightarrow 3)- β -D-Glcp-(1 \rightarrow residues [23]. The cross-peak at $\delta_{\text{C}}/\delta_{\text{H}}$ 3.37/69.45 ppm is assigned to \rightarrow 3,6)- β -D-Glcp-(1 \rightarrow [45–47]. The signal at $\delta_{\text{C}}/\delta_{\text{H}}$ 4.91/97.87 ppm is associated with \rightarrow 6)- β -D-Glcp-(1 \rightarrow [47]. Similarly, the cross-peaks at $\delta_{\text{C}}/\delta_{\text{H}}$ 4.12/68.78 and 3.77/68.59 ppm are assigned to H-5/C-5 and H-6/C-6 of \rightarrow 6)- β -D-Manp-(1 \rightarrow residues [23]. The $\delta_{\text{C}}/\delta_{\text{H}}$ 4.69/102.55 ppm signal is associated with \rightarrow 3)- β -D-Galp-(1 \rightarrow [45]. Additionally, the $^1\text{H}/^{13}\text{C}$ chemical shifts at $\delta_{\text{C}}/\delta_{\text{H}}$ 4.44/102.74 and 3.25/73.08 ppm are assigned to C1-H and C2-H of (1 \rightarrow 4)-linked β -D-xylan [44].

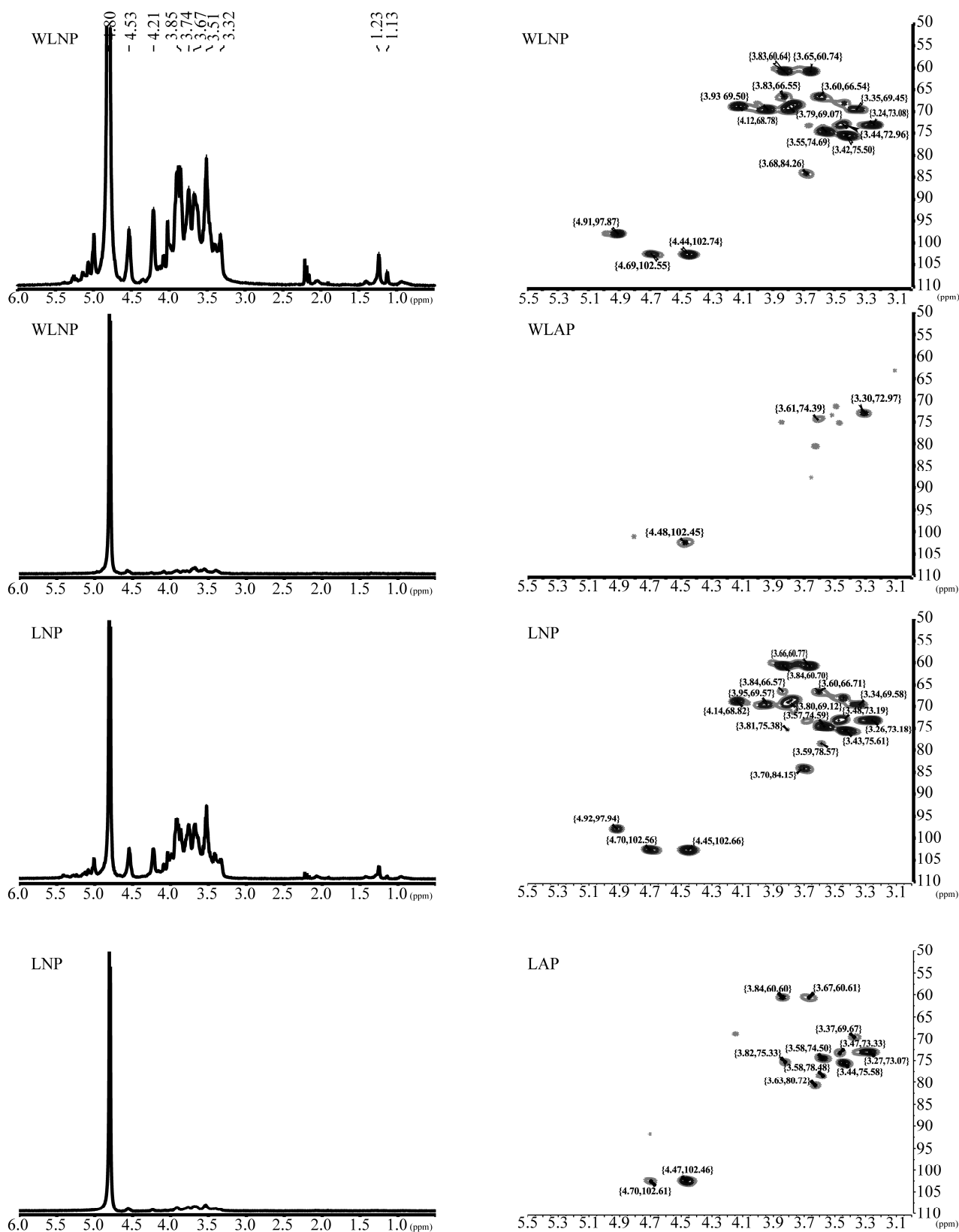


Figure 6. ^1H (left) and HSQC (right) NMR spectra of WLNP (white Lingzhi neutral polysaccharide), WLAP (white Lingzhi acidic polysaccharide), LNP (Lingzhi neutral polysaccharide), and LAP (Lingzhi acidic polysaccharide).

In summary, the neutral polysaccharides from white Lingzhi and Lingzhi were found to be composed of (1 → 4) α -glucan, \rightarrow 3)- β -D-Glcp-(1 →, \rightarrow 3,6)- β -D-Glcp-(1 →, \rightarrow 6)- β -D-Glcp-(1 →, \rightarrow 6)- β -D-Manp-(1 →, \rightarrow 3)- β -D-Galp-(1 →, and (1 → 4)-linked β -D-xylan. This is consistent with the information obtained from the FTIR spectrum. The spectra of WLNP and LNP are very similar, with the exception that LNP has an additional peak (δ_C/δ_H 3.70/84.15 ppm) representing \rightarrow 3,6)- β -D-Galp-(1 → [45]. This indicates that LNP has an additional branch type, which may have an impact on its functionality. In comparison to the neutral polysaccharides, the structure of the acidic polysaccharides, particularly WLAP, appears to be simpler.

3.5.5. Antioxidant Activities

The polysaccharide concentration of white Lingzhi significantly exceeded that of Lingzhi. *Ganoderma* polysaccharides had different antioxidant patterns for different free radicals, and the properties of the four polysaccharides varied slightly (Figure 7). There was no significant difference in the scavenging effect of the four polysaccharides on H_2O_2 or Fe^{2+} , and it was obviously dose-dependent. However, the dose required to scavenge H_2O_2 was much smaller. WLNP was the most effective in scavenging DPPH radicals at concentrations between 1 and 4 mg/mL.

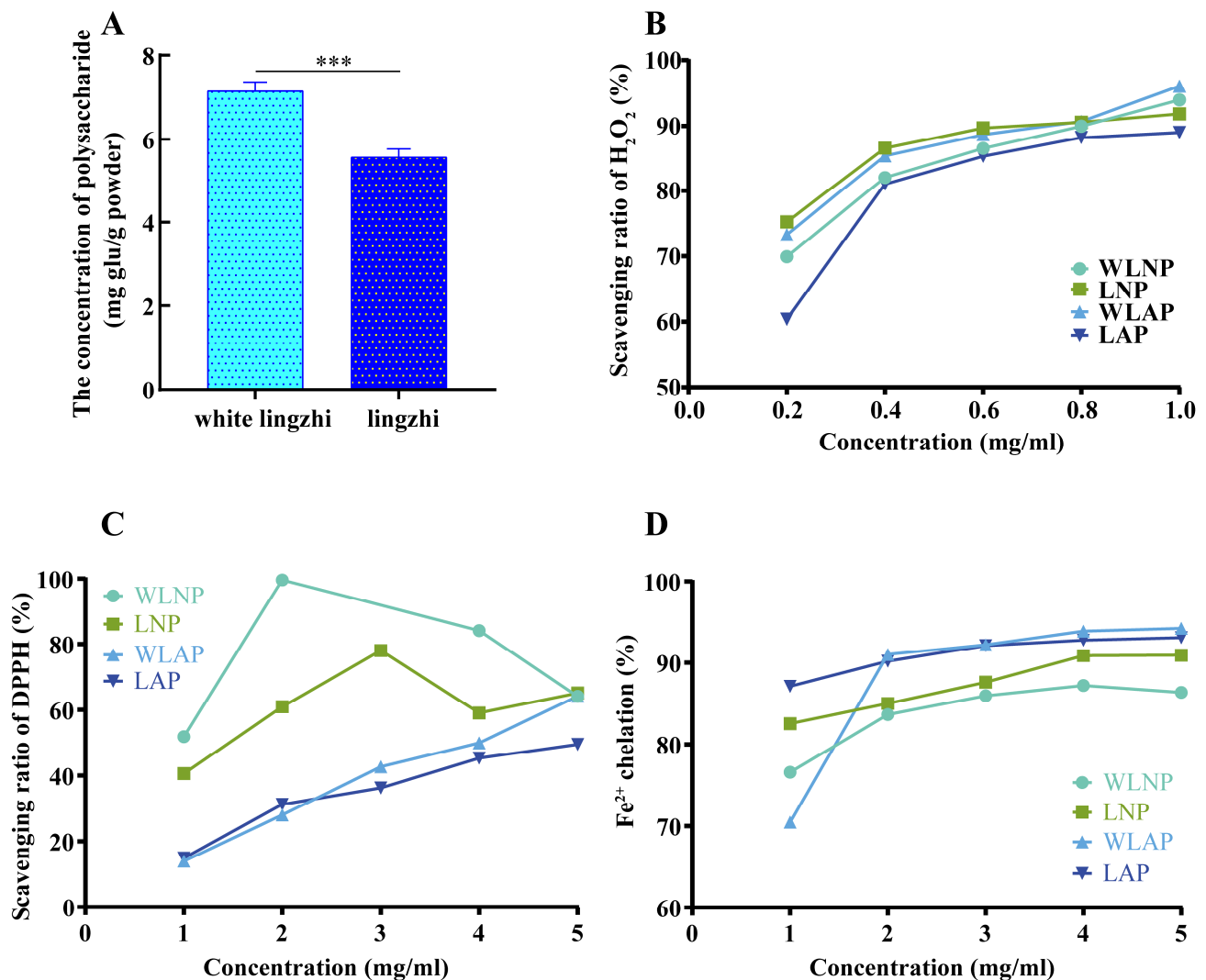


Figure 7. Concentrations and antioxidant activities of polysaccharides. The concentration (A) of polysaccharides and capacity to scavenging DPPH (B), H_2O_2 (C) and chelate Fe^{2+} (D) in white Lingzhi and Lingzhi. *** indicates that $p < 0.001$.

4. Discussion

We compared the antioxidant activities of several components of *Ganoderma*, among which polysaccharides were the strongest, suggesting that the antioxidant activities in white Lingzhi and Lingzhi may be derived mostly from their polysaccharides.

Neutral and acidic polysaccharides of high Mw ($>10^5$ Da) were obtained from our extractions. *Ganoderma* polysaccharides with larger or smaller Mw have been obtained [48,49], which could be related to different varieties, extractions, and purification procedures [50]. The relationships between Mw and antioxidant activity were inconclusive. One viewpoint is that Mw in polysaccharides is positively correlated with its bioactivity [51]. However, some studies have shown that degraded polysaccharides have stronger antioxidant activity [49]. The two outcomes may not be contradictory. A possible explanation is that the antioxidant activity of polysaccharides shows two peaks in the molecular weight distribution. Another explanation is that the antioxidant activity of the purified polysaccharides can be positively correlated with Mw, and degradation further enhances their activity.

In light of the intended applications of these polysaccharide extracts, their stability must be considered. Polysaccharides must be subjected to intense heat in certain manufacturing processes. High thermal stability suggests that polysaccharides can be used for functionalization and many other chemical modifications [52] to enhance their biological activity. Additionally, the high stability of polysaccharides can reduce the costs associated with storage and transportation. The application scenario of a polysaccharide depends on its water retention and stability. For example, heat-stable acidic polysaccharides can be used in food processing, while neutral polysaccharides with good water retention can be added to cosmetics.

Reactive oxygen species (ROS) are reactive molecules produced by normal metabolism in the human body. Excessive levels of ROS can cause many metabolic disorders and diseases, such as cancer, liver injury, coronary heart disease, and hypertension [53]. Therefore, the balance between the production and removal of ROS is crucial to human health. Many studies have reported that polysaccharides can alleviate oxidative damage by scavenging free radicals, such as Sanqi polysaccharide, *Agaricus bisporus* polysaccharide, and *G. lucidum* polysaccharide [54–56]. The four kinds of *Ganoderma* polysaccharides have clear antioxidant activities. Although the antioxidant effect of WLNP is only slightly higher than that of LNP, the concentrations of triterpenoids and total phenolics in white Lingzhi are significantly higher. Similarly to polysaccharides, these triterpenoids and phenolics can also scavenge ROS [19]. And, our results showed that the triterpenoids and phenolics of white Lingzhi were superior to Lingzhi in antioxidant activity. Overall, the effective doses of white Lingzhi may be smaller than those of Lingzhi, which should reduce undesirable side effects.

The structure of polysaccharides is critically associated with their activity. Heteropolysaccharides exhibit superior anti-tumor and immunomodulatory properties because they contain a variety of monosaccharides [57]. Mannose, one of the most critical components, can activate the immune response effectively by mediating the mannose receptor [58]. Neutral residues like $\rightarrow 3$)- β -D-Galp-(1 \rightarrow and $\rightarrow 3,6$)- β -D-Galp-(1 \rightarrow may suggest a compositional basis for anti-aging activity [59].

We must comprehensively consider the efficacy and taste of *G. lucidum* because it is well established in Chinese traditional medicine. It is clear that the taste of Lingzhi reduces its consumption. Researchers are working on methods to reduce the bitterness and make Lingzhi better suited to consumer needs [42]. Our analysis of amino acid composition showed that the relative proportions of bitter amino acids did not differ between white Lingzhi and Lingzhi, but in absolute terms were higher in white Lingzhi, as were its triterpenoid. But, people who consume white Lingzhi agree that it is less bitter, contradicting previous studies reporting that bitterness was attributed to the content of triterpenoids [60]. Here, the ratio of triterpenoids to proteins (T/P) was introduced to represent the bitterness. Although the triterpenoid and protein levels in white Lingzhi were higher than those in Lingzhi, the T/P was significantly lower (the value of T/P was

0.58 for white Lingzhi and 0.64 for Lingzhi). Protein is often tasteless but may interfere with taste buds' perception of white Lingzhi as less bitter [61].

5. Conclusions

In conclusion, the differences in the nutritional and medicinal ingredients of white Lingzhi and Lingzhi were compared. There is little difference in the nutritional ingredients of the two *Ganoderma*, but the concentrations of the medicinal ingredients in white Lingzhi are higher than those in Lingzhi. The triterpenoid levels in white Lingzhi are 20% higher than those in Lingzhi, and the polysaccharide fraction is 28% higher. White Lingzhi neutral polysaccharide has better antioxidant activity than do the other three polysaccharides, with one less branch than the Lingzhi neutral polysaccharide. The factors that affect the taste of *G. lucidum* are complex, and we use the ratio of triterpenoid to protein (T/P) to track the degree of bitterness. The T/P value of Lingzhi is 10% higher than that of white Lingzhi, which may help explain why white Lingzhi has a less bitter taste. Our findings provide a basis for the commercialization and further development of white Lingzhi.

Author Contributions: P.W.: data curation, formal analysis, investigation, methodology, resources, and writing—original draft. F.F.: data curation, formal analysis, investigation, methodology, resources, writing—original draft, and writing—review and editing. C.Y.: data curation, formal analysis, investigation, methodology, resources, and validation. Q.T.: data curation, formal analysis, investigation, methodology, and resources. G.T.: data curation, formal analysis, and writing—review and editing. L.H.: data curation, formal analysis, and writing—original draft. Y.B.: formal analysis and writing—review and editing. Q.L.: conceptualization, data curation, formal analysis, funding acquisition, investigation, methodology, project administration, resources, supervision, validation, writing—original draft, and writing—review and editing. All authors have read and agreed to the published version of the manuscript.

Funding: This research was funded by Yunnan Liu Qinghong Specialist Station (202305AF150164).

Data Availability Statement: The original contributions presented in the study are included in the article, further inquiries can be directed to the corresponding author.

Conflicts of Interest: The authors declare no conflicts of interest.

References

- Jin, X.; Ruiz Beguerie, J.; Sze, D.M.; Chan, G.C. *Ganoderma lucidum* (Reishi mushroom) for cancer treatment. *Cochrane Database Syst. Rev.* **2016**, *4*, Cd007731. [\[CrossRef\]](#) [\[PubMed\]](#)
- Liu, X.; Xu, Y.; Li, Y.; Pan, Y.; Sun, Z.; Zhao, S.; Hou, Y. *Ganoderma lucidum* fruiting body extracts inhibit colorectal cancer by inducing apoptosis, autophagy, and G0/G1 phase cell cycle arrest in vitro and in vivo. *Am. J. Transl. Res.* **2020**, *12*, 2675–2684. [\[PubMed\]](#)
- Lin, Z.B. Cellular and molecular mechanisms of immuno-modulation by *Ganoderma lucidum*. *J. Pharmacol. Sci.* **2005**, *99*, 144–153. [\[CrossRef\]](#)
- Wu, S.J.; Zhang, S.Y.; Peng, B.; Tan, D.C.; Wu, M.Y.; Wei, J.C.; Wang, Y.T.; Luo, H. *Ganoderma lucidum*: A comprehensive review of phytochemistry, efficacy, safety and clinical study. *Food Sci. Hum. Wellness* **2024**, *13*, 568–596. [\[CrossRef\]](#)
- Ahmad, M.F.; Ahmad, F.A.; Zeyauallah, M.; Alsayegh, A.A.; Mahmood, S.E.; AlShahrani, A.M.; Khan, M.S.; Shama, E.; Hamouda, A.; Elbendary, E.Y.; et al. *Ganoderma lucidum*: Novel insight into hepatoprotective potential with mechanisms of action. *Nutrients* **2023**, *15*, 1874. [\[CrossRef\]](#)
- Wang, J.; Cao, B.; Zhao, H.; Feng, J. Emerging roles of *Ganoderma lucidum* in anti-aging. *Aging Dis.* **2017**, *8*, 691–707. [\[CrossRef\]](#)
- Ma, H.T.; Hsieh, J.F.; Chen, S.T. Anti-diabetic effects of *Ganoderma lucidum*. *Phytochemistry* **2015**, *114*, 109–113. [\[CrossRef\]](#)
- Li, T.H.; Hu, H.P.; Deng, W.Q.; Wu, S.H.; Wang, D.M.; Tsering, T. *Ganoderma leucocontextum*, a new member of the *G. lucidum* complex from southwestern China. *Mycoscience* **2015**, *56*, 81–85. [\[CrossRef\]](#)
- Chen, H.; Zhang, J.; Ren, J.; Wang, W.; Xiong, W.; Zhang, Y.; Bao, L.; Liu, H. Triterpenes and meroterpenes with neuroprotective effects from *Ganoderma leucocontextum*. *Chem. Biodivers.* **2018**, *15*, e1700567. [\[CrossRef\]](#)
- Gao, X.; Qi, J.; Ho, C.T.; Li, B.; Mu, J.; Zhang, Y.; Hu, H.; Mo, W.; Chen, Z.; Xie, Y. Structural characterization and immunomodulatory activity of a water-soluble polysaccharide from *Ganoderma leucocontextum* fruiting bodies. *Carbohydr. Polym.* **2020**, *249*, 116874. [\[CrossRef\]](#)
- Batra, P.; Sharma, A.K.; Khajuria, R. Probing Lingzhi or Reishi medicinal mushroom *Ganoderma lucidum* (higher Basidiomycetes): A bitter mushroom with amazing health benefits. *Int. J. Med. Mushrooms* **2013**, *15*, 127–143. [\[CrossRef\]](#) [\[PubMed\]](#)
- Klupp, N.L.; Kiat, H.; Bensoussan, A.; Steiner, G.Z.; Chang, D.H. A double-blind, randomised, placebo-controlled trial of *Ganoderma lucidum* for the treatment of cardiovascular risk factors of metabolic syndrome. *Sci. Rep.* **2016**, *6*, 29540. [\[CrossRef\]](#)

13. Chen, X.; Hu, Z.P.; Yang, X.X.; Huang, M.; Gao, Y.; Tang, W.; Chan, S.Y.; Dai, X.; Ye, J.; Ho, P.C.; et al. Monitoring of immune responses to a herbal immuno-modulator in patients with advanced colorectal cancer. *Int. Immunopharmacol.* **2006**, *6*, 499–508. [\[CrossRef\]](#)
14. Chu, T.T.; Benzie, I.F.; Lam, C.W.; Fok, B.S.; Lee, K.K.; Tomlinson, B. Study of potential cardioprotective effects of *Ganoderma lucidum* (Lingzhi): Results of a controlled human intervention trial. *Br. J. Nutr.* **2012**, *107*, 1017–1027. [\[CrossRef\]](#)
15. Nascimento, F.d.S.; Santos, C.A.F.; Figueiredo Neto, A.; Bezerra, L.G.V.; da Silva, S.A.M.F. Crude proteion content in pigeon pea grain lines. *Rev. Contemp.* **2024**, *4*, e3615. [\[CrossRef\]](#)
16. Fraile-Fabero, R.; Ozcariz-Fermoselle, M.V.; Oria-de-Rueda-Salgueiro, J.A.; Garcia-Recio, V.; Cordoba-Diaz, D.; Del P Jiménez-López, M.; Gírbés-Juan, T. Differences in antioxidants, polyphenols, protein digestibility and nutritional profile between *Ganoderma lingzhi* from industrial crops in asia and *Ganoderma lucidum* from cultivation and Iberian origin. *Foods* **2021**, *10*, 1750. [\[CrossRef\]](#) [\[PubMed\]](#)
17. Fountoulakis, M.; Lahm, H.W. Hydrolysis and amino acid composition of proteins. *J. Chromatogr. A* **1998**, *826*, 109–134. [\[CrossRef\]](#) [\[PubMed\]](#)
18. Gao, J.Z.; Fang, H. Spectrophotometric determination of L-tryptophan by condensation with p-dimethylaminobenzaldehyde. *J. Cap. Norm. Univ.* **1999**, *1999*, 48–52.
19. Oludemi, T.; Barros, L.; Prieto, M.A.; Heleno, S.A.; Barreiro, M.F.; Ferreira, I. Extraction of triterpenoids and phenolic compounds from *Ganoderma lucidum*: Optimization study using the response surface methodology. *Food Funct.* **2018**, *9*, 209–226. [\[CrossRef\]](#)
20. Heleno, S.A.; Barros, L.; Martins, A.; Queiroz, M.; Santos-Buelga, C.; Ferreira, I. Fruiting body, spores and in vitro produced mycelium of *Ganoderma lucidum* from Northeast Portugal: A comparative study of the antioxidant potential of phenolic and polysaccharidic extracts. *Food Res. Int.* **2012**, *46*, 135–140. [\[CrossRef\]](#)
21. Ding, J.; Du, H.; Tan, H.; Li, J.; Wang, L.; Li, L.; Zhang, Y.; Liu, Y. Optimization of protein removal process of *Lonicera japonica* polysaccharide and its immunomodulatory mechanism in cyclophosphamide-induced mice by metabolomics and network pharmacology. *Food Sci. Nutr.* **2022**, *11*, 364–378. [\[CrossRef\]](#) [\[PubMed\]](#)
22. Yuan, Z.; Cong, G.; Zhang, J. Effects of exogenous salicylic acid on polysaccharides production of *Dendrobium officinale*. *S. Afr. J. Bot.* **2014**, *95*, 78–84. [\[CrossRef\]](#)
23. Feng, X.; Wang, P.; Lu, Y.; Zhang, Z.; Yao, C.; Tian, G.; Liu, Q. A novel polysaccharide from *Heimioporus retisporus* displays hypoglycemic activity in a diabetic mouse model. *Front. Nutr.* **2022**, *9*, 964948. [\[CrossRef\]](#) [\[PubMed\]](#)
24. Sun, L.; Wang, C.; Shi, Q.; Ma, C. Preparation of different molecular weight polysaccharides from *Porphyridium cruentum* and their antioxidant activities. *Int. J. Biol. Macromol.* **2009**, *45*, 42–47. [\[CrossRef\]](#)
25. Chen, Y.; Xue, Y. Purification, chemical characterization and antioxidant activities of a novel polysaccharide from *Auricularia polytricha*. *Int. J. Biol. Macromol.* **2018**, *120*, 1087–1092. [\[CrossRef\]](#)
26. Yu, Z.; Liu, L.; Xu, Y.; Wang, L.; Teng, X.; Li, X.; Dai, J. Characterization and biological activities of a novel polysaccharide isolated from raspberry (*Rubus idaeus* L.) fruits. *Carbohydr. Polym.* **2015**, *132*, 180–186. [\[CrossRef\]](#) [\[PubMed\]](#)
27. Wang, P.; Feng, X.; Lv, Z.; Liu, J.; Teng, Q.; Chen, T.; Liu, Q. Temporal dynamics of lignin degradation in *Quercus acutissima* sawdust during *Ganoderma lucidum* cultivation. *Int. J. Biol. Macromol.* **2024**, *268*, 131686. [\[CrossRef\]](#) [\[PubMed\]](#)
28. Abeygunawardana, C.; Williams, T.C.; Sumner, J.S.; Hennessey, J.P., Jr. Development and validation of an NMR-based identity assay for bacterial polysaccharides. *Anal. Biochem.* **2000**, *279*, 226–240. [\[CrossRef\]](#)
29. Ganie, S.A.; Haq, E.; Masood, A.; Hamid, A.; Zargar, M.A. Antioxidant and protective effect of ethyl acetate extract of *podophyllum hexandrum* rhizome on carbon tetrachloride induced rat liver injury. *Evid.-Based Complement. Altern. Med.* **2011**, *2011*, 238020. [\[CrossRef\]](#)
30. Li, C.; Huang, Q.; Fu, X.; Yue, X.J.; Liu, R.H.; You, L.J. Characterization, antioxidant and immunomodulatory activities of polysaccharides from *Prunella vulgaris* Linn. *Int. J. Biol. Macromol.* **2015**, *75*, 298–305. [\[CrossRef\]](#)
31. Dinis, T.C.P.; Madeira, V.M.C.; Almeida, L.M. Action of phenolic derivatives (acetaminophen, salicylate, and 5-aminosalicylate) as inhibitors of membrane lipid peroxidation and as peroxy radical scavengers. *Arch. Biochem. Biophys.* **1994**, *315*, 161–169. [\[CrossRef\]](#) [\[PubMed\]](#)
32. Stojković, D.S.; Barros, L.; Calhelha, R.C.; Glamočlija, J.; Ćirić, A.; van Griensven, L.J.; Soković, M.; Ferreira, I.C. A detailed comparative study between chemical and bioactive properties of *Ganoderma lucidum* from different origins. *Int. J. Food Sci. Nutr.* **2014**, *65*, 42–47. [\[CrossRef\]](#) [\[PubMed\]](#)
33. Liang, X.; Hu, Q.; Wang, X.; Li, L.; Dong, Y.; Sun, C.; Hu, C.; Gu, X. Thermal kinetics of a lignin-based flame retardant. *Polymers* **2020**, *12*, 2123. [\[CrossRef\]](#)
34. Rozi, P.; Abuduwaili, A.; Mutailifu, P.; Gao, Y.; Rakhmanberdieva, R.; Aisa, H.A.; Yili, A. Sequential extraction, characterization and antioxidant activity of polysaccharides from *Fritillaria pallidiflora* Schrenk. *Int. J. Med. Mushrooms* **2019**, *131*, 97–106. [\[CrossRef\]](#)
35. Zhao, H.; Li, H.; Lai, Q.; Yang, Q.; Dong, Y.; Liu, X.; Wang, W.; Zhang, J.; Jia, L. Antioxidant and hepatoprotective activities of modified polysaccharides from *Coprinus comatus* in mice with alcohol-induced liver injury. *Int. J. Biol. Macromol.* **2019**, *127*, 476–485. [\[CrossRef\]](#)
36. Liu, D.; Sun, Q.; Xu, J.; Li, N.; Lin, J.; Chen, S.; Li, F. Purification, characterization, and bioactivities of a polysaccharide from mycelial fermentation of *Bjerkandera fumosa*. *Carbohydr. Polym.* **2017**, *167*, 115–122. [\[CrossRef\]](#)
37. Seedeve, P.; Moovendhan, M.; Viramani, S.; Shanmugam, A. Bioactive potential and structural chracterization of sulfated polysaccharide from seaweed (*Gracilaria corticata*). *Carbohydr. Polym.* **2017**, *155*, 516–524. [\[CrossRef\]](#) [\[PubMed\]](#)

38. Wang, H.; Gao, T.; Du, Y.; Yang, H.; Wei, L.; Bi, H.; Ni, W. Anticancer and immunostimulating activities of a novel homogalacturonan from *Hippophae rhamnoides* L. berry. *Carbohydr. Polym.* **2015**, *131*, 288–296. [\[CrossRef\]](#)
39. Bociek, S.M.; Welti, D. The quantitative analysis of uronic acid polymers by infrared spectroscopy. *Carbohydr. Res.* **1975**, *42*, 217–226. [\[CrossRef\]](#)
40. Yang, J.P.; Hsu, T.; Lin, F.; Hsu, W.; Chen, Y. Potential antidiabetic activity of extracellular polysaccharides in submerged fermentation culture of *Coriolus versicolor* LH1. *Carbohydr. Polym.* **2012**, *90*, 174–180. [\[CrossRef\]](#)
41. Jiang, J.; Kong, F.; Li, N.; Zhang, D.; Yan, C.; Lv, H. Purification, structural characterization and in vitro antioxidant activity of a novel polysaccharide from *Boshuzhi*. *Carbohydr. Polym.* **2016**, *147*, 365–371. [\[CrossRef\]](#) [\[PubMed\]](#)
42. Ru, Y.; Chen, X.; Wang, J.; Guo, L.; Lin, Z.; Peng, X.; Qiu, B.; Wong, W.-L. Structural characterization, hypoglycemic effects and mechanism of a novel polysaccharide from *Tetrastigma hemsleyanum* Diels et Gilg. *Int. J. Med. Mushrooms* **2019**, *123*, 775–783. [\[CrossRef\]](#) [\[PubMed\]](#)
43. Wang, W.F.; Stevenson, A.; Reuter, D.C.; Sirota, J.M. Absolute band intensities in the ν_{19}/ν_{23} (530 cm^{-1}) and ν_7 (777 cm^{-1}) bands of acetone ((CH_3)₂CO) from 232 to 295 K. *Spectrochim. Acta Part A Mol. Biomol. Spectrosc.* **2000**, *56*, 1111–1116. [\[CrossRef\]](#)
44. Li, M.F.; Fan, Y.M.; Xu, F.; Sun, R.C. Structure and thermal stability of polysaccharide fractions extracted from the ultrasonic irradiated and cold alkali pretreated bamboo. *J. Appl. Polym. Sci.* **2011**, *121*, 176–185. [\[CrossRef\]](#)
45. Choi, J.W.; Synytsya, A.; Capek, P.; Bleha, R.; Pohl, R.; Park, Y.I. Structural analysis and anti-obesity effect of a pectic polysaccharide isolated from Korean mulberry fruit Oddi (*Morus alba* L.). *Carbohydr. Polym.* **2016**, *146*, 187–196. [\[CrossRef\]](#)
46. Kono, H.; Kondo, N.; Hirabayashi, K.; Ogata, M.; Totani, K.; Ikematsu, S.; Osada, M. NMR spectroscopic structural characterization of a water-soluble β -(1→3, 1→6)-glucan from *Aureobasidium pullulans*. *Carbohydr. Polym.* **2017**, *174*, 876–886. [\[CrossRef\]](#) [\[PubMed\]](#)
47. Liu, X.; Liu, D.; Chen, Y.; Zhong, R.; Gao, L.; Yang, C.; Ai, C.; El-Seedi, H.R.; Zhao, C. Physicochemical characterization of a polysaccharide from *Agroclype aegirita* and its anti-ageing activity. *Carbohydr. Polym.* **2020**, *236*, 116056. [\[CrossRef\]](#)
48. Ooi, L.S.M.; Ooi, V.E.C.; Fung, M.C. Induction of gene expression of immunomodulatory cytokines in the mouse by a polysaccharide from *Ganoderma lucidum* (Curt.: Fr.) P. Karst. (Aphyllophoromycetidae). *Int. J. Med. Mushrooms* **2002**, *4*, 27–35. [\[CrossRef\]](#)
49. Xu, Y.; Zhang, X.; Yan, X.H.; Zhang, J.L.; Wang, L.Y.; Xue, H.; Jiang, G.C.; Ma, X.T.; Liu, X.J. Characterization, hypolipidemic and antioxidant activities of degraded polysaccharides from *Ganoderma lucidum*. *Int. J. Biol. Macromol.* **2019**, *135*, 706–716. [\[CrossRef\]](#)
50. Yang, Y.; Qiu, Z.; Li, L.; Vidyarthi, S.K.; Zheng, Z.; Zhang, R. Structural characterization and antioxidant activities of one neutral polysaccharide and three acid polysaccharides from *Ziziphus jujuba* cv. *Hamidazao*: A comparison. *Carbohydr. Polym.* **2021**, *261*, 117879. [\[CrossRef\]](#)
51. Kang, Q.; Chen, S.; Li, S.; Wang, B.; Liu, X.; Hao, L.; Lu, J. Comparison on characterization and antioxidant activity of polysaccharides from *Ganoderma lucidum* by ultrasound and conventional extraction. *Int. J. Biol. Macromol.* **2019**, *124*, 1137–1144. [\[CrossRef\]](#) [\[PubMed\]](#)
52. Xu, C.; Yang, C.; Mao, D. Fraction and chemical analysis of antioxidant active polysaccharide isolated from flue-cured tobacco leaves. *Pharmacogn. Mag.* **2014**, *10*, 66–69. [\[CrossRef\]](#) [\[PubMed\]](#)
53. Ma, J.S.; Liu, H.; Han, C.-R.; Zeng, S.J.; Xu, X.J.; Lu, D.J.; He, H.J. Extraction, characterization and antioxidant activity of polysaccharide from *Pouteria campechiana* seed. *Carbohydr. Polym.* **2020**, *229*, 115409. [\[CrossRef\]](#) [\[PubMed\]](#)
54. Feng, S.L.; Cheng, H.R.; Xu, Z.; Feng, S.C.; Yuan, M.; Huang, Y.; Liao, J.Q.; Ding, C.B. Antioxidant and anti-aging activities and structural elucidation of polysaccharides from *Panax notoginseng* root. *Process Biochem.* **2019**, *78*, 189–199. [\[CrossRef\]](#)
55. Li, S.; Liu, H.; Wang, W.; Wang, X.; Zhang, C.; Zhang, J.; Jing, H.; Ren, Z.; Gao, Z.; Song, X.; et al. Antioxidant and anti-aging effects of acidic-extractable polysaccharides by *Agaricus bisporus*. *Int. J. Biol. Macromol.* **2018**, *106*, 1297–1306. [\[CrossRef\]](#)
56. Ma, C.; Feng, M.; Zhai, X.; Hu, M.; You, L.; Luo, W.; Zhao, M. Optimization for the extraction of polysaccharides from *Ganoderma lucidum* and their antioxidant and antiproliferative activities. *J. Taiwan Inst. Chem. Eng.* **2013**, *44*, 886–894. [\[CrossRef\]](#)
57. Ruthes, A.C.; Smiderle, F.R.; Iacomini, M. Mushroom heteropolysaccharides: A review on their sources, structure and biological effects. *Carbohydr. Polym.* **2016**, *136*, 358–375. [\[CrossRef\]](#)
58. Zhu, X.-L.; Lin, Z.-b. Effects of *Ganoderma lucidum* polysaccharides on proliferation and cytotoxicity of cytokine-induced killer cells. *Acta Pharmacol. Sin.* **2005**, *26*, 1130–1137. [\[CrossRef\]](#)
59. Liang, X.; Liu, M.; Wei, Y.; Tong, L.; Guo, S.; Kang, H.; Zhang, W.; Yu, Z.; Zhang, F.; Duan, J.-a. Structural characteristics and structure-activity relationship of four polysaccharides from *Lycii fructus*. *Int. J. Biol. Macromol.* **2023**, *253*, 127256. [\[CrossRef\]](#)
60. Hennenke, F.; Cheikh-Ali, Z.; Liebisch, T.; Maciá-Vicente, J.G.; Bode, H.B.; Piepenbring, M. Distinguishing commercially grown *Ganoderma lucidum* from *Ganoderma lingzhi* from Europe and East Asia on the basis of morphology, molecular phylogeny, and triterpenic acid profiles. *Phytochemistry* **2016**, *127*, 29–37. [\[CrossRef\]](#)
61. Bohin, M.C.; Roland, W.S.; Gruppen, H.; Gouka, R.J.; van der Hijden, H.T.; Dekker, P.; Smit, G.; Vincken, J.P. Evaluation of the bitter-masking potential of food proteins for EGCG by a cell-based human bitter taste receptor assay and binding studies. *J. Agric. Food Chem.* **2013**, *61*, 10010–10017. [\[CrossRef\]](#) [\[PubMed\]](#)

Disclaimer/Publisher’s Note: The statements, opinions and data contained in all publications are solely those of the individual author(s) and contributor(s) and not of MDPI and/or the editor(s). MDPI and/or the editor(s) disclaim responsibility for any injury to people or property resulting from any ideas, methods, instructions or products referred to in the content.